Available online at www.sciencedirect.com
SCIENCE DIRECT
Talanta 68 (2006) 653–658
Talanta
www.elsevier.com/locate/talanta

Direct electrochemistry and superficial characterization of DNA-cytochrome *c*-MUA films on chemically modified gold surface

Xiaoqin Ding, Jingbo Hu *, Qilong Li

Department of Chemistry, Beijing Normal University, Beijing 100875, China

Received 8 December 2004; received in revised form 10 May 2005; accepted 10 May 2005
Available online 17 June 2005

Abstract

Cytochrome *c* (Cyt. *c*) was immobilized on the 11-mercaptohendecanoic acid (MUA)-modified gold electrode. The electrode was stable and sensitive to Cyt. *c*. Later, DNA was also immobilized on the two-layer modified electrode. Cyclic voltammetry studies show that Cyt. *c* can interact with dsDNA and ssDNA. The binding site sizes were determined to be 15 base pairs per Cyt. *c* molecule with dsDNA and 30 nucleotides binding 1 Cyt. *c* molecule with ssDNA. The modified electrodes were characterized by quartz crystal microbalance (QCM), impedance spectroscopy and atomic force microscope (AFM). The modified electrode can be used for determining DNA.

Keywords: Electrochemistry; Superficial characterization; Cytochrome *c*; DNA; Gold electrode

1. Introduction

Cytochrome *c* (Cyt. *c*) plays a major role in electron-transport in biochemical transformations. It is a water-soluble heme protein that exists in the cytosol between the inner and outer membranes of mitochondria. Under physiological conditions, it transfers electrons between cytochrome *c* reductase and cytochrome *c* oxidase, which are both embedded in the mitochondrial membrane. Reversible electron transfer between electrode and redox proteins immobilized in films provides a basis for constructing biosensors, biomedical devices, and enzymatic bioreactors [1,2]. It is difficult for cytochrome *c* to exhibit a voltammetric response at a bare electrode because of its extremely slow electron-transfer kinetics at the electrode/solution interface. It usually shows a short-lived and transient response on a metal surface [3,4]. Since the direct electron transfer of cytochrome *c* was first observed [4,5], problems remain whereby cytochrome *c* molecules form irreversible adsorption blocks on the electrode surface, or where protein molecules unfolding on adsorption onto the electrode surfaces lead to poisoning and deactivation of a bare electrode [6,7]. Many important developments have taken place in the design and structural characterization of electrode surfaces. The idea of an electrode's surface having a specific adsorption interaction that can be modified to enhance the electron transfer rate of cytochrome *c* has been proposed, e.g. using 4,4′-bipyridyl, mercapto, or disulfide [8–15], and pyridinethio [16]. And many articles have described the electrochemistry of cytochrome *c* in terms of self-assembled monolayers (SAMs)-modified electrode [17–20]. Direct electron transfer between a protein (the redox active group) and an electrode can serve as a model system to help understand electron transfer mechanisms in biological systems. DNA is a molecule that acts as a form of memory storage for genetic information. DNA is also present in mitochondria. The interaction of DNA with metal proteins can be used in the analysis of electroactive metal proteins. The investigation of the interaction between DNA and other biomolecules is of great importance in life science.

This article reports the direct electron transfer of cytochrome *c* immobilized onto the MUA-modified gold electrode. Furthermore, the electrochemistry of DNA adsorbed cytochrome *c*/MUA/Au was investigated and the interaction between cytochrome *c* and DNA was also studied. The binding site sizes were determined to be 15 base

* Corresponding author. Tel.: +86 10 62209398; fax: +86 10 58802075.
E-mail address: hujingbo@bnu.edu.cn (J. Hu).

0039-9140/$ – see front matter © 2005 Elsevier B.V. All rights reserved.
doi:10.1016/j.talanta.2005.05.009

pairs per Cyt. *c* molecule with dsDNA and 30 nucleotides binding 1 Cyt. *c* molecule with ssDNA. The modified electrode was characterized by quartz crystal microbalance (QCM), impedance spectroscopy and atomic force microscope (AFM).

2. Experimental

2.1. Apparatus

2.1.1. Electrochemical experiments

Electrochemical experiments were carried out using CHI-660 electrochemical system. A conventional three-electrode configuration was used for all electrochemical experiments. The three-electrode configuration was composed of a modified gold working electrode, an Ag/AgCl[$KCl_{(sat)}$] reference electrode and a platinum wire auxiliary electrode. Cyclic voltammetry on electrodes coated with Cyt. *c* and DNA was done in buffers containing no Cyt. *c*.

2.1.2. AFM measurements

AFM images were obtained by AutoProbe CP Rsearch Scanning Probe Microscope (Park Scientific Instruments, CA). IC-AFM mode and Ultravlevers 20 were used. p-Type silicon wafers (1 0 0) were used as the substrate for the preparation of the thin films. Au thin films were deposited on the oxidized silicon wafer by electron beam evaporation at 10^{-6} Torr and room temperature. Thickness of the films was monitored by a temperature stabilized quartz thickness gauge during the deposition. The gold film thickness was controlled to be 25 Å.

2.1.3. QCM measurements

The working electrode for QCM (Chenhua, Shanghai, China) measurements was a 7.995 MHz AT-cut quartz crystal with gold electrodes. The diameter of the quartz crystal was 13.7 mm, and the diameter of gold electrode was 5 mm.

2.1.4. Impedance spectroscopy measurements

Faradic impedance measurements were performed in the presence of 10 mM $K_3[Fe(CN)_6]/K_4[Fe(CN)_6]$ (1:1)-mixture as a redox-probe, using alternating voltage, 10 mV. Impedance measurements were performed at a bias potential of 0.22 V in the frequency range 100 kHz to 0.1 Hz. The impedance spectra were plotted in the form of complex plane diagrams (Nyquist plots). The experiment impedance data were analyzed by the Kramers–Kroeing procedure to confirm true frequency-dependence impedance. The experiment impedance spectra were simulated using electronic equivalent circuits.

2.2. Reagents

Horse heart cytochrome *c* (Sigma) was dissolved in 1.0 mM pH 6.03 K_2HPO_4–KH_2PO_4 buffer solution (PBS). 11-Mercaptopropionic acid (MUA, Sigma) was also dissolved in 1.0 mM pH 7.9 PBS solution. Native double-stranded fish sperm DNA (dsDNA, Sigma) was used as received and dissolved in 0.05 M NaCl–0.005 M Tris buffer prior to use. Denatured single-stranded DNA (ssDNA) was produced by heating a dsDNA solution in a water bath at 100 °C for about 5 min followed by rapid cooling in an ice bath. The supporting electrolyte was 0.05 mM pH 7.0 PBS buffer solution. All reagents were of analytical reagent grade. Triply distilled water was used throughout.

2.3. Preparation of modified electrodes

The area ($0.0226 \pm 0.005\ cm^2$) of the gold electrode was determined from the charge associated with gold oxide reduction in 1 M H_2SO_4. Gold electrode was first polished with 0.05 μm alumina polishing suspension and then cleaned ultrasonically in water and ethanol, respectively, for 3 min. The freshly polished electrode was scanned over the potential range of 0.0–1.5 V in 1 M H_2SO_4 until a constant voltammogram was obtained. Then the electrode was rinsed with water and dipped into 1.5 mM MUA solution for about 22 h. Later, it was immersed into 6 μM Cyt. *c* solution for 25 min and rinsed with water. The process is also illustrated in Scheme 1. Finally, a droplet of DNA solution was transferred onto the electrode surface for some time. After rinsing and drying with a stream of nitrogen, the electrode was put in the electrochemical cell in the presence of 0.05 mM pH 7.0 PBS solution.

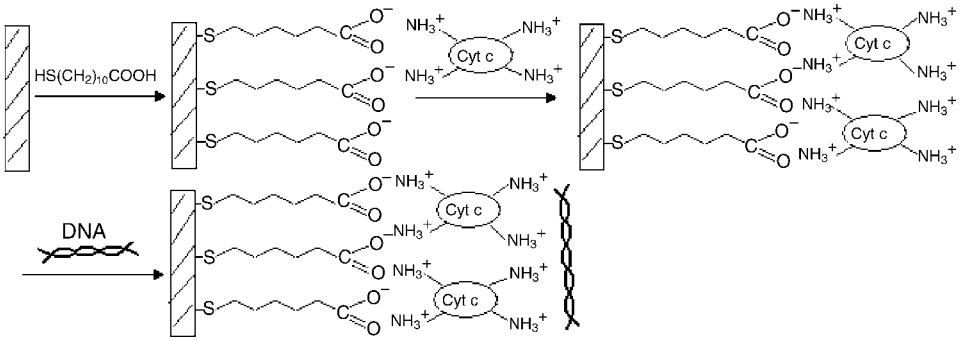

Scheme 1. The surface assembly of Cytochrome c and DNA at a MUA-modified gold electrode.

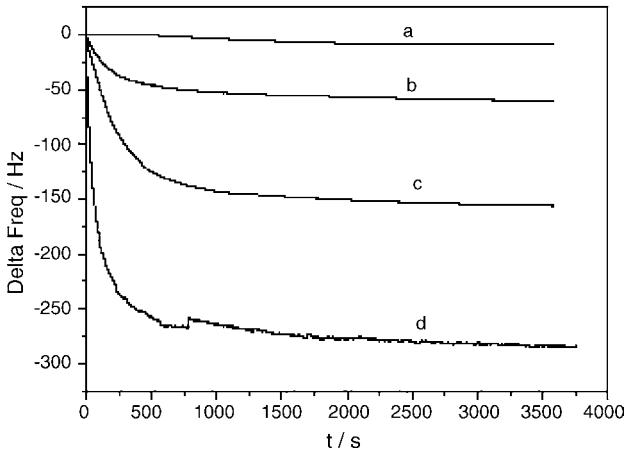

Fig. 1. Frequency response on time for different modified electrodes. (a) Bare gold electrode in PBS solution; (b) MUA self-assembly from PBS solution onto electrode; (c) Cyt. *c* attachment onto MUA-modified electrode; (d) immobilization of DNA. c_{MUA} = 1.5 mM, pH_{MUA} 7.9, $c_{Cyt.\,c}$ = 6 μM, $pH_{Cyt.\,c}$ 6.03, c_{DNA} = 33.7 μM.

3. Results and discussion

3.1. Quartz crystal microbalance characterization

As mentioned above, MUA, Cyt. *c* and DNA were gradually immobilized on the quartz crystal. The modified quartz crystals were rinsed with water and dried in ambient nitrogen before QCM characterization. Fig. 1 shows the frequency changes upon the formations of different films. Using the Sauerbrey equation, (Eq. (1)), [21] where f_0 is the basic crystal frequency and A is the apparent area of the quartz microbalance electrode. Under these conditions, a decrease in frequency of 1 Hz results from a mass increase of 1.38 ng provided that the frequency shifts are due exclusively to adsorption of material on the QCM resonator. The frequency changes of crystal upon interaction with a MUA solution corresponds to Δf = 50.5 Hz, so the surface coverage of the MUA units was estimated to be 1.6×10^{-9} mol/cm^2. After treatment with Cyt. *c* solution, the frequency change of the crystal is higher. For a bulk concentration of Cyt. *c* corresponding to 6 μM, the crystal frequency change Δf = 90.25 Hz, which translates to a surface coverage of the Cyt. *c* monolayer of 5.05×10^{-11} mol/cm^2. As DNA was immobilized on the crystal, the frequency further decreased. From these results we can conclude that MUA, Cyt. *c* and DNA were all immobilized on the gold electrode.

$$\Delta f = -\frac{2.26 f_0^2 \Delta m}{A} \quad (1)$$

3.2. Atomic force microscope characterization

AFM images were taken to investigate changes of the surface morphology of the Au film before and after the immobilizations of MUA, Cyt. *c* and DNA. To confirm the immobilization, the following procedures were also carried out. Au thin films were immersed in a 1.5 mM MUA solution for 22 h. As the treatment with Cyt. *c* and DNA described above, the films were rinsed with water and dried in ambient nitrogen before AFM investigation. AFM images (Fig. 2) showed that the bare Au thin films had a typical discrete metal island structure. When MUA was immobilized on the Au films, the three-dimensional images changed slightly. After treatment with Cyt. *c*, the images change obviously. A protein layer on the Au/MUA film surface can be clearly observed. On the other hand, some polymers of Cyt. *c* appeared at the same time. The filose particles can be seen clearly when DNA was immobilized on the Au films. These AFM images indicate that MUA, Cyt. *c* and DNA were all immobilized onto gold electrode surface and changed the morphology of the surface more or less. They give us a clear impression about the structures of the films.

3.3. Impedance analysis

Fig. 3 shows the results of Faradic impedance spectroscopy on a bare gold electrode (curve a), MUA monolayer-modified electrode (curve b), MUA/Cyt. *c* two-layer modified electrode (curve c) and MUA/Cyt. *c*/DNA three-layer modified electrode (curve d) in the presence of redox probe $Fe(CN)_6^{4-/3-}$ measured at the formal potential. It can be seen that the bare gold electrode exhibits an almost straight line that is characteristic of a diffusional limiting step of the electrochemical process. The impedance spectra follow the theoretical shapes and include a semicircle portion, observed at higher frequencies, which correspond to the electron transfer limited process, followed by a linear part characteristic of the lower frequency attributable to a diffusionally limited electron transfer. It can be seen that the diameter of semicircle at the high frequency increases upon the stepwise formation of modifier to the electrode surface. The respective semicircle diameters correspond to the electron transfer resistance at the electrode surface. The self-assemble monolayers produce ordered, tightly packed films that decrease electroactivity of solution probes. Such layers can be expected to present a considerable Ohmic resistance, which should be indicated by the impedance spectrum irrespective of the effect on electron-transfer of the redox pair. On the other hand, self-assembly MUA monolayer on the electrode surface generates a negatively charged surface which reduces the ability of the electrolyte to penetrate the layer, and eventually eliminates effectively the response of the $Fe(CN)_6^{4-/3-}$ anion. The immobilization of protein introduces the insulating protein layer on the assembled surface, which increases the diameter of the semicircle, implying a high electron transfer resistance. After DNA was immobilized, the electrode surface becomes more negative due to the negative DNA bone, which makes the diameter of the semicircle increases distinctly.

The equivalent circuit for an electrode undergoing heterogeneous electron transfer is usually described on the basis of the model by Randles as shown in Scheme 2. The circuit includes the ohmic resistance (R_s) of the electrolyte

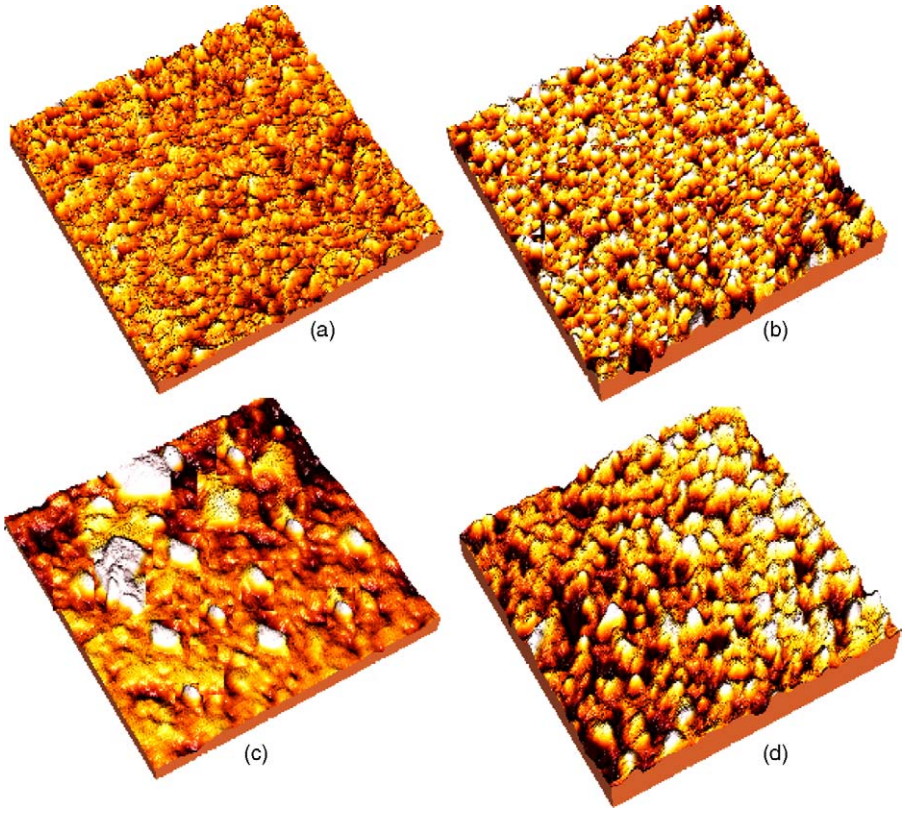

Fig. 2. The three-dimension AFM images of the different films electrodes. c_{MUA} = 1.5 mM, pH_{MUA} 7.9, $c_{Cyt.\,c}$ = 6 μM, $pH_{Cyt.\,c}$ 6.03, c_{DNA} = 33.7 μM. (a) Au; (b) Au/MUA; (c) Au/MUA/Cyt. *c*; (d) Au/MUA/Cyt. *c*/dsDNA.

solution, Warburg impedance (Z_w), resulting from the diffusion of ions to the interface from the bulk of the electrolyte, double-layer capacitance (C_{dl}) and electron transfer resistance (R_{et}). The two components of the scheme, R_s and Z_w, represent bulk properties of the electrolyte solution and diffusion of the applied redox probe. Thus, they are not affected by chemical transformations occurring at the electrode interface. The other two components of the circuit, C_{dl} and R_{et}, depend on the dielectric and insulating features at the electrode/electrolyte interface. We use this equivalent circuit to fit the impedance spectroscopy and determine C_{dl} and R_{et}. The electron transfer resistance of MUA/Au electrode is 389 kΩ (a), indicating assembly of MUA on the electrode surface generating a tightly packed film that introduces a barrier to the interfacial electron transfer. The immobilization of Cyt. *c* results in a clear increase of R_{et} (438.8 kΩ, b), due to gen-

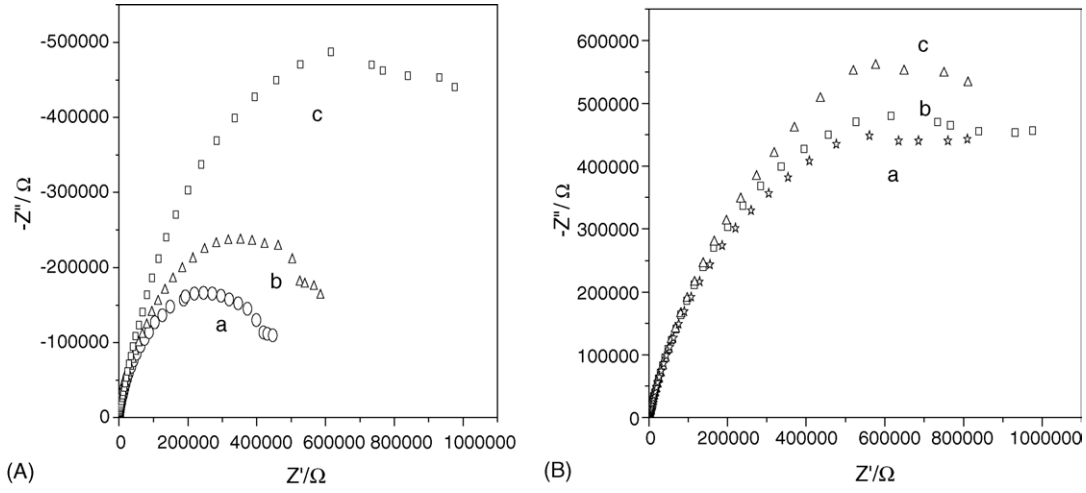

Fig. 3. Complex impedance plots Z′ vs. −Z″ at 220 mV vs. Ag/AgCl in 0.1 M KCl + 10 mM $Fe(CN)_6^{4-/3-}$ solution at: (A)—(a) MUA-modified electrode, (b) Cyt. *c*/MUA-modified electrode and (c) DNA/Cyt. *c*/MUA-modified electrode; (B)—(a) c_{DNA} = 1.95 μM, (b) c_{DNA} = 3.36 μM and (c) c_{DNA} = 19.5 μM. The frequency range is between 0.1 and 100,000 Hz with signal amplitude of 10 mV.

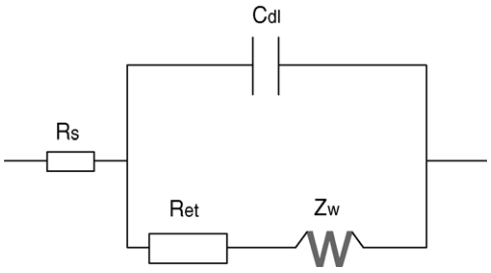

Scheme 2. Equivalent circuit used to model impedance data in the presence of redox couples.

erating an insulating protein layer on the electrode surface. After immobilization of DNA, the resistance increased from 438.8 to 907 kΩ (c). The value of R_{et} in last process is very large compared with earlier steps, which mean that effect of immobilization of DNA is very obvious. From Fig. 3B, we also can see that the change value of impedance increased with increasing the concentration of DNA.

3.4. Electrochemical properties of Cyt. c at the different modified electrodes

A typical cyclic voltammogram of Cyt. *c* is shown in Fig. 4. It is clear that a well-defined redox wave of Cyt. *c* was observed at the Au/MUA/Cyt. *c*-modified electrode with the reductive peak potential at 0.040 V, the corresponding oxidative peak potential at 0.083 V and $\Delta E_p = 43$ mV (Fig. 4Ac), but no voltammetric responses were observed at bare gold electrode (Fig. 4Aa). As discussed previously, the Au/MUA/Cyt. *c*/DNA-modified electrode was obtained through treatment with DNA solution. The formal potential of Cyt. *c* at Au/MUA/Cyt. *c*/DNA surface shifted negatively and the peak current of Cyt. *c* decreased (Fig. 4Ac), suggesting the presence of interactions between the Au/MUA/Cyt. *c* and DNA. As the isoelectric point of Cyt. *c* is 10.5, Cyt. *c* molecules could be strongly bound by its positive amino

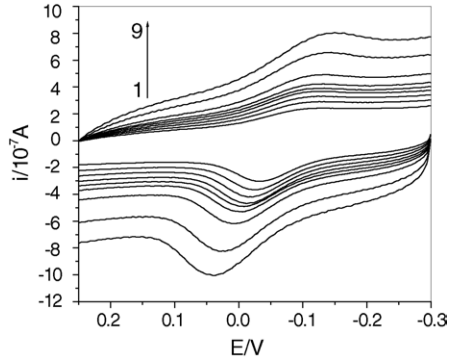

Fig. 5. Changes in the CV response of Au/MUA/Cyt. *c*/DNA with scan rate in a 0.05 mM pH 7.0 PBS solution. $c_{MUA} = 1.5$ mM, pH_{MUA} 7.9, $c_{Cyt.\,c} = 6$ μM, $pH_{Cyt.\,c}$ 6.03, $c_{DNA} = 33.7$ μM. Curves 1–9: scan rate = 0.05, 0.1, 0.15, 0.2, 0.25, 0.3, 0.35, 0.4 and 0.5, respectively.

groups through electrostatic interaction to negative phosphate groups along the DNA strand. We also can arrive at the same conclusion through DPV results (Fig. 4B).

The total amount of DNA adsorbed onto Au/MUA/Cyt. *c*/DNA surfaces can be determined from the coulometric charge associated with the oxidation of the adsorbed bases which gives rise to an irreversible cyclic voltammetric peak at +0.9 to ∼+1.0 V in a 0.1 mol/l pH 7.0 PBS solution [22]. From such measurements we obtained values of $\Gamma_{dsDNA} = 1.52 \times 10^{-10}$ mol/cm^2 (in base pairs) and $\Gamma_{ssDNA} = 2.94 \times 10^{-10}$ mol/cm^2 (in nucleotides), respectively. Combining these with the surface coverage values of the Cyt. *c*, the ratio of base pairs of the dsDNA to Cyt. *c* on the surface was determined to be ∼15 that is, 15 base pairs bind 1 Cyt. *c* molecule. For the ssDNA, the ratio of nucleotides to Cyt. *c* immobilized on the electrode surface was calculated to be ∼30, which means that 30 nucleotides bind 1 molecule of Cyt. *c*.

There was a good linearity in the change value of peak current with scan rate from 0.05 to 0.5 V/s (Fig. 5).

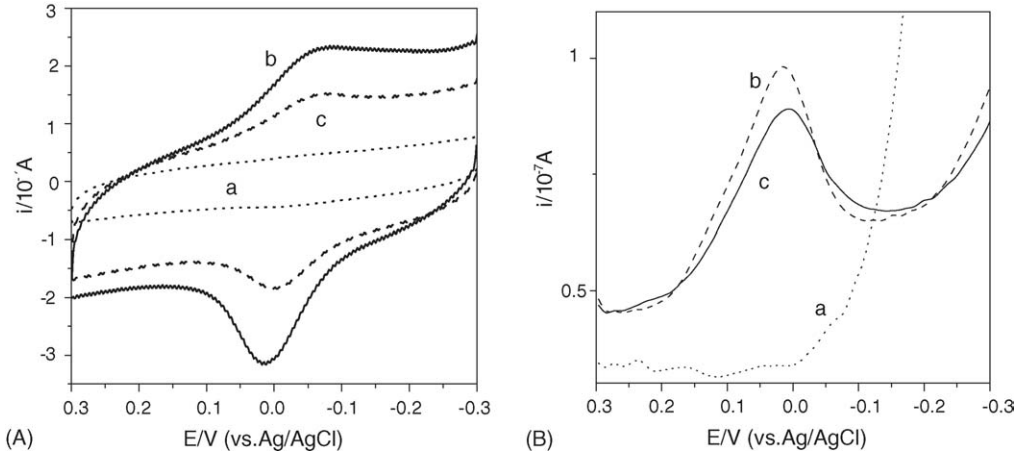

Fig. 4. Cyclic voltammograms (A) and differential pulse voltammograms (B) of Cyt. *c* at the different modified gold electrodes in a 0.05 mM pH 7.0 PBS solution. $c_{MUA} = 1.5$ mM, pH_{MUA} 7.9, $c_{Cyt.\,c} = 6$ μM, $pH_{Cyt.\,c}$ 6.03, $c_{DNA} = 33.7$ μM, Scan rate = 0.3 V/s. (a) Bare gold electrode; (b) Au/MUA/Cyt. *c* electrode; (c) Au/MUA/Cyt. *c*/DNA electrode.

The result is characteristics of an adsorption-controlled process.

3.5. Analytical application

The effect of equilibration time that controls a variable delay during which the Au/MUA/Cyt. *c*-modified electrode treated with DNA solution was studied. Equilibration times (ET) of 20, 25, 30, 35, 40, 50 and 60 min were applied to the course and the corresponding cyclic voltammograms were recorded. The results show the change of the current increased with increasing the accumulation time and then tended to level off, indicating that the adsorption equilibrium had been achieved. When the time exceeded 40 min the response began decreasing. So 35 min was chosen as optimum ET value. The temperature also affects the interaction between Cyt. *c* and DNA. Temperatures of 10, 20, 25, 30, 35 and 38 °C were controlled and the results suggest temperature greater than 35 °C have no considerable effect on the peak current and 35 °C was chosen as optimum temperature. Under the optimum conditions, the concentration of DNA can be determined according to the current change value of Cyt. *c* after treatment with DNA. Over two DNA concentration ranges of 0.0334–3.34 μM and 3.34–33.4 μM, the change value of the peak current increased linearly with the concentration of DNA. The modified electrode can be used for determining DNA.

4. Conclusions

Immobilizations of Cyt. *c* and DNA have been carried out on the Au/MUA electrode. Quartz crystal microbalance, impedance spectroscopy and AFM investigations show the method is applicable. From the direct electrochemistry of Cyt. *c* at the modified electrode, the binding sites sizes with dsDNA and ssDNA were explored. Additionally, DNA/Cyt. *c*/MUA/Au electrodes can be used to determine DNA quantitatively.

Acknowledgement

We are grateful to the National Natural Science Foundation of China (No. 20275007) for the provision of financial support.

References

[1] F.A. Armstrong, H.A. Hill, N.J. Walton, Acc. Chem. Res. 21 (1988) 407.
[2] M.F. Chaplin, C. Bucke, Enzyme Technology, Cambridge University Press, Cambridge, UK, 1990.
[3] P. Yeh, T. Kuwana, Chem. Lett. (1977) 1145.
[4] M.J. Eddowes, H.A.O. Hill, J. Chem. Soc. Chem. Commun. (1977) 771.
[5] P. Yeh, T. Kuwana, Chem. Lett. (1977) 1145.
[6] H.A.O. Hill, N.I. Hunt, A.M. Bond, J. Electroanal. Chem. 436 (1997) 17.
[7] A. Szucs, G.D. Hitchens, J.O. Bockris, Electrochim. Acta 37 (1992) 403.
[8] M.J. Eddowes, H.A.O. Hill, J. Am. Chem. Soc. 101 (1979) 4461.
[9] F.A. Armstrong, H.A.O. Hill, N.J. Walton, Acc. Chem. Res. 21 (1988) 40.
[10] F.A. Armstrong, H.A.O. Hill, N.J. Walton, J. Electroanal. Chem. 178 (1984) 69.
[11] Z.Q. Feng, S. Imabayashi, T. Kakiuchi, K. Niki, J. Electroanal. Chem. 394 (1995) 149.
[12] J.M. Sevilla, T. Pineda, A.J. Roman, R. Madueno, M. Blazquez, J. Elecroanal. Chem. 451 (1998) 89.
[13] Y. Sato, F. Mizutani, J. Electroanal. Chem. 473 (1999) 99.
[14] S. Dong, J. Li, Bioelectrochem. Bioenerg. 42 (1997) 7.
[15] Y. Zhou, T. Nagaoko, G. Zhu, Biophys. Chem. 79 (1999) 55.
[16] I. Taniguchi, S. Yoshimoto, M. Yoshida, S.I. Kobayashi, T. Miyawaki, Y. Aono, Y. Sunatsuki, H. Taira, Electrochim. Acta 45 (2000) 2843.
[17] C.X. Cai, J. Electroanal. Chem. 393 (1995) 119.
[18] N. Nakashima, Y. Miyata, M. Tominaga, Chem. Lett. (1996) 731.
[19] H. Ohno, K.I. Kato, Chem. Lett. (1998) 407.
[20] W. Qian, J.H. Zhuang, Y.H. Wang, Z.X. Huang, J. Electroanal. Chem. 447 (1998) 187.
[21] D. Laurent, B. Schlenoff, Langmuir 13 (1997) 1552.
[22] D. Pang, H.D. Abruna, Anal. Chem. 72 (2002) 4700.